

LOCOMOTION OF IN-PLANE ROBOT WITH CONTINUOUSLY SLIDING FEET

DAVID ZARROUK

*Dept. of Mechanical Engineering, Ben Gurion University,
Beer Sheva, Israel*

ANDREW PULLIN, RONALD S. FEARING

*Dept. of EECS, UC Berkeley
Berkeley, CA, USA*

This paper analyzes the in-plane locomotion of a minimally actuated dynamic hexapedal robot with continuously sliding feet. We formulate the fore-aft velocity of the robot as a function of the length of the legs, step angle, actuation frequency and the incline of the surface and compare this model to a nearly-flat experimental robot. The results are in good agreement with the model which shows that the progress of the robot is substantially reduced over slopes. The cost of transport of the robot is lower than other robots of its size.

1. Introduction

The interest in multi-legged crawling robots has been motivated by the demand for high-speed robust mechanisms capable of crawling over slippery and rough surfaces for a variety of applications ranging from reconnaissance to search and rescue. But slipping of the legs in the fore-aft and lateral directions has not been thoroughly examined. Many examples of miniature crawling robots, some of which are capable of running at more than ten body lengths per second can be found in the literature, such as Mini-Whegs [10], DASH [3], iSprawl [9], and STAR [15]. Multiple studies used the spring loaded inverted pendulum model (SLIP) of robot behavior in two dimensions [2]. Horizontal In-plane models which neglect vertical oscillation but are useful for steering and yaw stability were investigated by Schmit and Holmes [11] and Kukillaya and Holmes [8] who studied the dynamic locomotion model of cockroaches, in which they assume that the legs fully stick to the surface. They developed the lateral leg spring model (LLS) in which the robot is modeled as a rigid body with massless compliant legs, and limited their analysis to in-plane dynamics. Recently, Zarrouk & Fearing suggested the sliding spring leg (SSL) model to describe in-plane locomotion where the legs are sliding (throughout the contact

with the surface) along the fore-aft direction and sideways [14]. In this work, we present experimental results of the SSL model for running over horizontal surfaces and up inclines and compare it to the mathematical model.

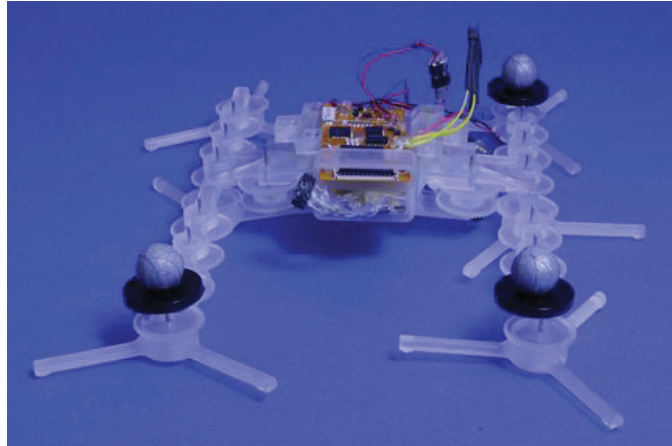


Figure 1. The experimental robot fitted with rigid legs. Its length is 120 mm and weighs 45 grams.

2. Robot model

In a traditional approach where sticking contact exists, it is possible to determine the robot motion by simply integrating the motor rotation and leg deformation to directly determine the position of the robot. However, this becomes impossible when the legs are sliding, as the relative velocity of the sliding legs relative to the ground is unknown.

2.1 *The robot*

The robot has a rigid body and six legs. Each side of the robot has 3 legs driven by a single motor where each leg is in 60° phase offset from the neighboring leg. Steering is achieved by differential velocity between the two sides. The yaw rate of the robot is measured using an onboard MEMS gyro and the velocity of the motors is estimated from back electromotive force (EMF). The length of the robot, including its legs is 160 mm and its total weight is 45 grams. A worm gear with a transmission ratio of 48:1 is used between the motor and the legs to ensure high torque output and relatively steady velocity.

2.2 Simplified model

Similarly to insects, the robot model runs with an alternating tripod gait consisting of a left tripod (LT, legs 1,4,5) and a right tripod (RT, legs 2,3,6). A step begins when a tripod contacts the surface and ends when it disengages, marking the beginning of the next step. A cycle is comprised of two successive steps LT and RT. The body of the robot is rigid with a mass m and inertia moment I relative to the center of mass (COM), which is assumed to be the geometrical center of the body. Assuming the robot runs in a straight line, the instantaneous velocity of the legs, rotating around their hips is

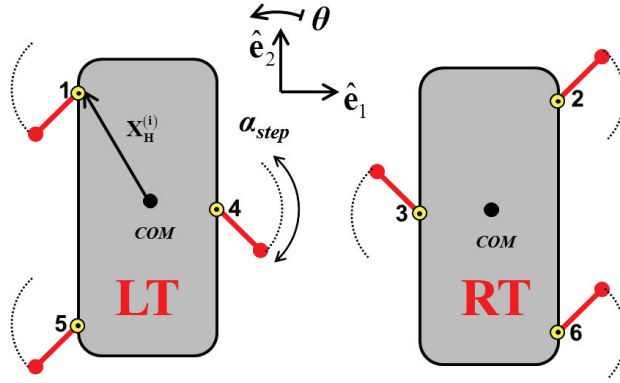


Figure 2. The Hexapod robot. LT is comprised of legs 1,4,5 and RT is made of legs 2,3,6.

$$\mathbf{V}_{leg} = \mathbf{V} + \dot{\alpha} \times \mathbf{L}_{leg} \quad (1)$$

where \mathbf{V}_{leg} is the vector velocity of the tips of the legs, \mathbf{V} is the velocity of the robot, $\dot{\alpha}$ is the angular velocity of the legs and \mathbf{L}_{leg} is the vector direction of the legs. The explicit values of the velocity of the legs in direction \mathbf{e}_1 and \mathbf{e}_2 are respectively

$$\begin{aligned} |V_{leg1}| &= \dot{\alpha} L_{leg} \sin(\alpha_0 - \dot{\alpha} t) \\ V_{leg2} &= V - \dot{\alpha} L \cos(\alpha_0 - \dot{\alpha} t) \end{aligned} \quad (2)$$

Where α_0 is the touchdown angle. The velocity V_{leg1} is independent of the velocity of the robot, where its sign depends on $\alpha = \alpha_0 - \dot{\alpha} t$ and on whether the leg is on the left or right side of the body. The thrust force of the robot is the sum of the components of the friction forces in the \mathbf{e}_2 direction.

$$F_{thrust} = -\mu_k \sum_i \left(F_n^{(i)} \frac{V_2^{(i)}}{V^{(i)}} \right) \quad (3)$$

When the robot is climbing a surface inclined by λ relative to the horizontal plane, the total normal force to the surface is $m g \cos(\lambda)$. If we assume that all the legs have a constant relative phase and are infinitely rigid, Eq. (3) becomes

$$F_{Thrust} = -m g \cos(\lambda) \mu_k \frac{V_2}{V} \quad (4)$$

or

$$F_{Thrust}(V) = \frac{-m g \cos(\lambda) \mu_k (V - \dot{\alpha} L_{leg} \cos(\alpha_0 - \dot{\alpha} t))}{\left(V^2 + (\dot{\alpha} L_{leg})^2 - 2 \dot{\alpha} L_{leg} \cos(\alpha_0 - \dot{\alpha} t) V \right)^{0.5}} \quad (5)$$

Using Newton's second law we can formulate the acceleration as a function of the velocity in the following ordinary differential equations (ODE)

$$\dot{V} = \frac{F_{Thrust}(V) + F_{ext}}{m} \quad (6)$$

Eq. (6) describes the velocity of the robot as a function of time. When the robot is climbing up a slope, the external force is due to its weight. In such case, Eq. (6) becomes

$$\dot{V} = \frac{F_{Thrust}(V) + F_{ext}}{m} = \frac{F_{Thrust}(V)}{m} - g \sin(\lambda) \quad (7)$$

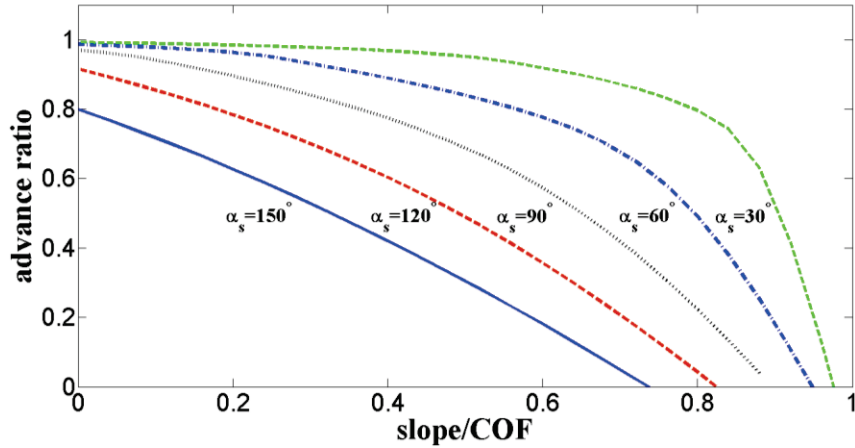


Figure 3. Advance ratio as a function of the slope divided by the COF for different step angles α_s .

Solving Eq. 7, it is possible to determine the advance ratio (defined as the ratio of the robot COM speed relative to the leg speed) as illustrated in figure 3. The advance ratio depends both on the step angle and on the slope. The robot cannot advance up a slope which is larger than its coefficient of friction.

3. Experiments

Our experimental setup consists of a hexapod robot which is similar to STAR [15], but with fixed sprawl angle. The position of the robot is measured using a Vicon multi camera tracking system. Our Vicon set up has 12 cameras which allow for sub-millimeter accuracy at 120Hz sampling rate.

3.1. *Measuring the leg to surface coefficient of friction*

During the experiments, the robot was run at roughly one third of its maximum speed. The contact angle between the plane of the legs and the surface is 7° (sprawl 83°) which allows for almost in-plane dynamics. As the angle between the legs and the surface is 7° only, the actual step angle of the robot was between 120° and 150° . The COF of the surface was measured by placing a cubical 3D printed part (same material as the legs) over the surface and changing the inclination until sliding is detected. Fifteen measurements were made to determine the COF of the surfaces. The friction angle, i.e. the angle of the slope over which sliding occurs, varied between 15 to 20 degrees on the wood and 15 to 25 degrees on the acrylic. Figure 4 shows that during locomotion on a horizontal surface, the legs slide mainly sideways.

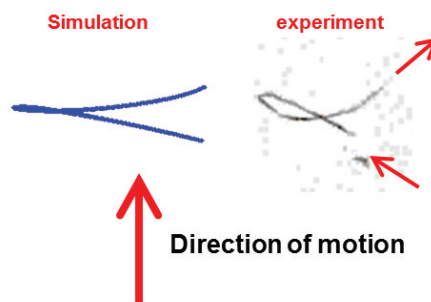


Figure 4. Footstep of a left leg of the robot in steady state running over a horizontal surface.

3.2. Climbing over a slope

Robot experiments were performed on plywood and acrylic. In each of the trials, the robot was run over a different slope. The slope was adjusted starting from a horizontal surface up to the stall angle of the robot. The velocity of the legs, as measured from the back EMF, was close to the input velocity. The difference, which was mainly due to the steering control (i.e. the robot slows down one side or another to keep going straight), was less than 5%. As a result, the different trials had practically the same actuation frequency. The advance ratios for the runs on wood and acrylic at zero incline are respectively 0.78 and 0.74, compared to 0.8 from the simulation, which is within the expected experimental error. Figure 5 presents the normalized advance ratio of the robot, defined as the ratio of the steady state velocity for a specific incline divided by the velocity for zero incline. The experiments are compared to our expected results from the simulation at a 150° step angle α_{step} . The velocity of the robot decreased almost linearly as a function of the slope as expected from the dynamics model. The experimental results with rigid legs are presented in the top two plots of Figure 18. Comparing those results to our analysis and simulation, we see a similar behavior where the velocity seems to be decreasing nearly as a linear function of the running surface incline slope.

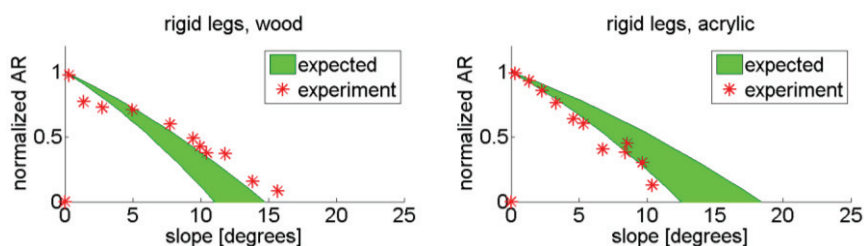


Figure 5. Normalized advance ratio of the robot as a function of the running surface incline slope for rigid and compliant legs on acrylic and wood surfaces. The range of the expected result is due to the uncertainties in the value of the friction coefficient.

4. Conclusions

The research described here focused on the analysis of in-plane hexapedal robotic locomotion. Explicitly, we investigate the locomotion of the robot and the thrust force it can generate as a function of the velocity. We start our analysis by formulating the relative velocity of the tips of the legs to the surface which allows us, based on the Coulomb model of friction, to determine the

resultant friction forces and thereby the forward thrust of the robot. For experimental validation, a purpose built robot with high, nearly flat, sprawl angle was developed to examine the in-plane mechanics model and simulation.

The advance ratio on inclined surfaces is a function of the slope and step angle but is independent of the actuation power and frequency. The advance ratio decreased monotonically with the slope. The robot performed slightly better than expected on the wooden surface and the stall angle over wood was found to be 17°. This may be attributable to the roughness of the surface which allows the tips of the legs to stick between the fibers of the wood. On acrylic, the robot performed slightly below the expected range and the stall angle is 12° only. The measured cost of transport (COT) of the robot on a horizontal surface (not including control board), which is the input energy to the motors divided by weight times distance is around 0.8 which is roughly half of the measured COT of similar size robots such as DASH [3]. This shows that this in-plane locomotion is relatively cost-effective even though the legs are continuously sliding, as the robot does not waste energy on undesired vertical oscillations.

In future work we will investigate the influence of leg compliance and concentrate on finding the cost of locomotion of the robots and analyzing stability under the different crawling conditions described in this manuscript.

References

- [1] B. Andrews, B. Miller, J. Schmitt, and J. E. Clark, "Running over unknown terrain with a one legged planar robot", *Bioinspiration and Biomimetics*. Vol. 6, doi:10.1088/1748-3182/6/2/026009, 2011.
- [2] R. Blickhan, R. J. Full, "Similarity in multilegged locomotion: Bouncing like a monopode". *J. Comparative Physiology A*. Vol. 173, No. 5, pp. 509-517, 1993.
- [3] P. Birkmeyer, K. Peterson, and R.S. Fearing, "DASH: A dynamic 16g hexapedal robot", IEEE Int. Conf. on Intelligent Robots and Systems, pp. 2683-2689, 2009.
- [4] J.G Cham, S.A. Bailey, J.E. Clark, R.J. Full, and M.R. Cutkosky, "Fast and robust: Hexapedal robots via shape deposition manufacturing", *The international Journal of Robotics Research*, Vol. 21, No. 10-11, pp. 869-882, 2002.
- [5] R. J. Full, T. Kubow, J. Schmitt, P. Holmes, and D. Koditschek, "Quantifying dynamic stability and maneuverability in legged locomotion", *Integrative and Comparative Biol.* Vol. 42, pp. 149-157, 2002.
- [6] P. Holmes, R. J. Full, D. Koditschek, J. Guckenheimer, " The dynamics

of legged locomotion: models, analyses and challenges", *SIAM Review*, Vol. 48, No. 2, pp. 207-304.

[7] D. L. Jindrich, and R. Full, "Dynamic stabilization of rapid hexapedal locomotion", *Journal of Exp. Biol.*, 205, pp. 2803-2823, 2002.

[8] R. P. Kuznetsov, P. Holmes, "A hexapedal jointed-leg model for insect locomotion in the horizontal plane", *Biol. Cyber.*, DOI 10.1007/s00422-007-0180-2, 2007.

[9] S. Kim, J. E. Clark, and M. R. Cutkosky, "iSprawl: Design and turning of high-speed autonomous open-loop running", *The Int. Journal of Robotic Research*, Vol. 25, No.9. pp. 903-912, 2006.

[10] J. M. Morrey, B. Lambrecht, A.D. Horchler, R. E. Ritzmann, and R.D. Quinn, "Highly mobile and robust small quadruped robots", *IEEE Int. Conf. on Intelligent Robots and Systems*, Vol. 1, pp. 82-87, 2003.

[11] J. Schmitt, P. Holmes, "Mechanical models for insect locomotion: dynamics and stability in the horizontal plane I. Theory", *Biol. Cyber.* Vol. 83, pp. 501-515, 2000.

[12] K. Tsujita, H. Toui, and K. Tsuchiya, "Dynamic turning control of a quadruped robot using nonlinear oscillators," *Proc. IEEE/RSJ Int. Conf. on Intelligent Robots and Systems*, pp. 969-974, 2004.

[13] J. D. Weingarten, G. A. D. Lopes, M. Buehler, R. E. Groff, and D. E. Koditschek, "Automated gait adaptation for legged robots", *IEEE Int. Conf. on Robotics and Automation*, pp. 2153-2158, 2004.

[14] D. Zarruk, R.S. Fearing, "Cost of transport of a dynamic hexapedal robot", *IEEE International Conference on Robotics and Automation 2013*.

[15] D. Zarruk, A. Pullin, N.J. Kohut, R.S. Fearing, "Sprawl tuned autonomous robot", *IEEE International Conference on Robotics and Automation 2013*.